

Cite this article as: Yang Fulai, Wang Qiang, Zhang Zheng. Evolution Characteristics of Microstructure and Twin in High-Cycle Fatigue of AZ31 Magnesium Alloy[J]. Rare Metal Materials and Engineering, 2023, 52(08): 2693-2701.

ARTICLE

# Evolution Characteristics of Microstructure and Twin in High-Cycle Fatigue of AZ31 Magnesium Alloy

Yang Fulai<sup>1</sup>, Wang Qiang<sup>2</sup>, Zhang Zheng<sup>1</sup>

<sup>1</sup> School of Materials Science and Engineering, Beihang University, Beijing 100191, China; <sup>2</sup> School of Materials Science and Engineering, North University of China, Taiyuan 030051, China

**Abstract:** Microstructure evolution and fracture morphology during high cycle fatigue in AZ31 magnesium alloy were investigated by fatigue test at different loading frequencies (3 and 30 Hz) and stress amplitudes (90, 95, 100, 105, 110 MPa). Electron back-scattered diffraction (EBSD) analysis results show that the number of residual twins in the matrix increases with the increase in loading stress, and the residual twins mainly exist in the form of  $\{10\bar{1}2\}$  tensile twins. Gradual grain refinement is observed with increasing stress amplitude, which is due to the grain refinement induced by the evolution of tensile twinning during fatigue deformation. The significant weakening of the texture strength with increasing stress amplitude is related to the recrystallization mechanism after fatigue deformation. Through the scanning electron microscope (SEM) analysis of the fatigue fracture, it is found that the fatigue crack initiation (FCI) occurs in twin layer, the area of the fatigue crack growth (FCG) in the specimen gradually decreases with the increase in stress, and obvious fatigue striations (FS) are observed in FCG. The final fracture (FF) is rough surface, and there are mainly tear ridges and dimples. The dimple is observed in the final fracture, and the size and number of dimples decrease with the increase in stress.

**Key words:** AZ31 magnesium alloy; high-cycle fatigue; twin; fracture morphology

As the lightest alloy with high specific strength, good casting properties, excellent ductility and corrosion resistance, AZ series magnesium alloys have received more and more attention and have been widely used in different fields<sup>[1]</sup>. Light-weighting is one of the key ways to improve fuel efficiency and reduce carbon dioxide emissions in vehicles, and has gradually become a core competitiveness standard for automotive companies<sup>[2-3]</sup>. Magnesium alloys have high strength-to-mass ratio, excellent vibration absorption, satisfying castability and machinability, and have been recognized as the lightest commercially available metal with great development potential in automotive industry<sup>[4-5]</sup>. So far, almost 90% of Mg alloy's non-load bearing products are manufactured by casting process<sup>[6-7]</sup>. Compared to as-cast magnesium alloy, wrought magnesium alloys have excellent properties and the material has outstanding advantages for applications in the automotive industry<sup>[8]</sup>. As automotive components are inevitably subjected to dynamic cyclic stresses during actual service and failure, it is necessary to study their fatigue fracture mechanisms to

ensure their service life. In recent years, a few studies have reported microstructure evolution after fatigue deformation.

Wen et al<sup>[9]</sup> investigated the microstructure evolution of AZ31 magnesium alloy during low cycle fatigue (LCF). The results show that at low strain amplitudes, fatigue deformation is dominated by dislocation slip and produces microcracks on the specimen surface; at high strain amplitude control conditions, the rate of crack growth increases. Matsuzuki et al<sup>[10]</sup> investigated the effect of microstructure evolution on the deformation of AZ31 magnesium alloy during low cycle fatigue test. Xu et al<sup>[11]</sup> investigated the effect of tensile twinning on the crack initiation mechanism of pure magnesium during fatigue. The results show that extruded magnesium alloys with strong basal texture are easy to produce tensile twins during tensile-compression loading. The cracks nucleate at the twin grain boundaries, initiate and then grow inward, leading to final fracture. The incompatibility of the twin boundaries with the matrix can be reduced by weakening the strong basal texture of the magnesium alloy. The fatigue crack initiation

Received date: March 06, 2023

Corresponding author: Yang Fulai, Ph. D., School of Materials Science and Engineering, Beihang University, Beijing 100191, P. R. China, E-mail: buaayangfulai@163.com

Copyright © 2023, Northwest Institute for Nonferrous Metal Research. Published by Science Press. All rights reserved.

resistance of magnesium alloy is improved. Yang et al<sup>[12]</sup> investigated the crack initiation mechanism of AZ31 magnesium alloy during the high cycle fatigue (HCF). The results show that the microcracks are often developed in the twinned region. Uematsu et al<sup>[13]</sup> investigated the effect of different stress amplitudes on the location of fatigue crack initiation. The results show that at low stress amplitude, the cracks mainly occur at the matrix stage. At high stress amplitude, the cracks mainly occur at the grain boundary. Tokaji et al<sup>[14]</sup> investigated the effect of fatigue propagation behaviour of AZ31 magnesium alloy at different extrusion rates and temperatures. The results show that the fatigue strength and anti-crack growth ability of AZ31B magnesium alloy increase with the decrease in extrusion temperature. The improvement of fatigue properties of magnesium alloy is mainly due to the effect of grain refinement, which accords with the Hal-Petch theory formula. Average grain diameter decreases and polycrystal yield strength increases. Yin et al<sup>[15]</sup> investigated the low cycle fatigue behaviour of AZ31 magnesium alloy using quasi-in-situ technique. The results of stress-strain hysteresis line show that there is a significant tensile-compressive asymmetry in the stress level in fatigue test, and significant cyclic hardening and cyclic softening are observed in *S-N* curves. The quasi-in-situ microstructure characterization indicates that the twin-texture behavior is the cause of these phenomena. Koike et al<sup>[16]</sup> investigated the high cycle fatigue behaviour of AZ31 magnesium alloy. The results show that as the stress amplitude increases, the tensile-compression asymmetry becomes more obvious in the stress-strain response curve. Abbas Jamali et al<sup>[17]</sup> investigated the effect of different grain sizes and different grain boundary misorientation angles on the fatigue crack initiation mechanism of AZ31 magnesium alloy. The results show that the grain boundary fracture with large misorientation angle and transcrystalline fracture between large grains are the main mechanism of fatigue crack initiation in AZ31 magnesium alloy with strong basal texture. Trojanova et al<sup>[18]</sup> investigated the fatigue behaviour of three Mg-Al-Zn alloys: AZ31, AZ91 and AZ63, under high frequency cyclic loading. The results show that AZ63 and AZ91 alloys contain discontinuous and continuous precipitation phases as well as intermetallic compound Mg<sub>17</sub>Al<sub>12</sub>, which may be crack initiation points. The specimens are gradually loaded at room temperature with increasing stress amplitude. The fatigue fracture behavior was analyzed using a scanning electron microscope (SEM). The cracks propagate from the surface of the specimen to the interior by branching in different directions and through the lamellar discontinuous precipitated phase. The important role of twinning and dislocation motion during high frequency cycling was discussed. Yu et al<sup>[19]</sup> investigated the microstructure evolution of Mg-6Zn-1Mn alloy during HCF. The results show that at high stress, twinning promotes fatigue deformation, and at low stress, twinning promotes recrystallization of Mg-6Zn-1Mn alloy at room temperature, gradually changing from twinning-dominated deformation to slip-dominated deformation. With the increase in the number

of cycles, the grain is refined and the texture of the strong base plane is weakened. Yang et al<sup>[20]</sup> attributed the fatigue cyclic of AZ31 magnesium alloy to deformation twinning. The effect of the number of loading cycles on the deformation mechanism is inconsistent. For better application of deformed magnesium alloys, there is an urgent need to investigate and to evaluate the fatigue mechanism of magnesium alloys.

In this study, the high cycle fatigue behaviour of AZ31 magnesium alloy sheets was investigated by fully reversed stress-controlled fatigue tests at different loading frequencies. The effects on the microstructural evolution under low and high frequency loading were compared. The effect of different loading frequencies on fatigue fracture behaviour was described by SEM characterization. Different loading cycles were used in the fatigue test, aiming to find out the fatigue pattern between the loading cycles and the microstructure of the magnesium alloy.

## 1 Experiment

The initial material used in this investigation was commercially AZ31 magnesium alloy rolled sheet with a thickness of 3 mm after homogenization, hot rolling deformation and stress relieving annealing, and the alloy composition is shown in Table 1.

The specimen is machined into a “bone bar” with a spacing of 25 mm, a thickness of 3.0 mm and a width of 10 mm, as shown in Fig. 1a. Tensile tests were performed using an Instron 3382 universal tensile tester and the strain rate was maintained at  $1.0 \times 10^{-3} \text{ s}^{-1}$  during the tests. Fatigue specimens were taken along the rolling direction (RD) as shown in Fig. 1b. Prior to the fatigue test, the specimens were sanded by progressively finer (#1000-#5000) SiC sandpaper until the surface of the specimens was smooth and free of obvious scratches to avoid surface defects caused by machining marks<sup>[21]</sup>.

Stress-controlled fatigue tests were performed on an Instron 8801 servo-hydraulic test machine under the same environmental conditions as the quasi-static tests. The fatigue tests were set at  $f=3 \text{ Hz}$  and  $f=30 \text{ Hz}$ , and the fatigue tensile-compressive stress ratio was  $R=-1$ . The stress amplitude was chosen from 90 MPa to 110 MPa with increments of 5 MPa. After fatigue fracture, the fracture area was cut from the cross-section and the fracture morphology was analyzed using SEM. The longitudinal section of the specimen fracture at different stress amplitudes was analyzed by EBSD.

## 2 Results and Discussion

### 2.1 Microstructure of the as-received materials

To analyze the grain size and microstructure evolution after fatigue deformation of rolled AZ31 alloy, the initial organization of the specimens characterized by EBSD and the microstructure of the metallographic observation specimens

**Table 1** Chemical composition of the AZ31 alloy (wt%)

Al	Zn	Mn	Si	Fe	Cu	Ni	Mg
2.5	0.7	0.2	0.3	0.005	0.05	0.005	Bal.

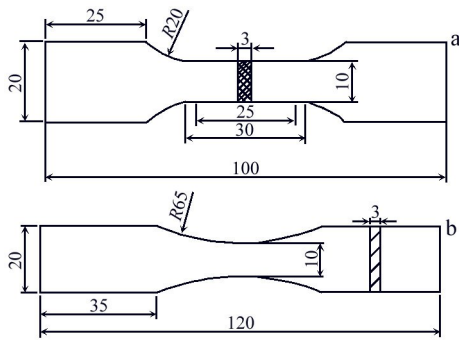


Fig.1 Size of tensile specimen (a) and fatigue specimen (b)

are shown in Fig. 2a and 2b. The microstructure of AZ31 magnesium alloy sheet consists of equiaxed crystals of unequal size. The AZ31 magnesium alloy sheet has fine and uniform grain size distribution, and the discontinuous dynamic recrystallization (DDRX) generated during deformation is the main reason for grain refinement. Fig. 2c shows the grain size distribution statistics, the grain size ranges from 2 μm to 25 μm, and the average grain size is about 9 μm.

Fig.2d shows the microscopic texture of AZ31 magnesium alloy sheet. The grains show a clear meritocratic orientation, with the *c*-axis of the grain perpendicular to the RD direction, forming a very strong basal texture component with a basal texture strength of MAX=13.65, which is a typical feature of rolled magnesium alloy sheet. The elliptic profile of the orientation distribution of the base plane indicates that  $\langle a \rangle$  slip is more likely to occur.

**2.2 Quasi-static behavior**

Fig. 3 shows the uniaxial tensile stress-strain curves of AZ31 alloy in different directions along the surface of the sheet, and the tensile strain rate is 0.001 s<sup>-1</sup>. As shown in the Fig.3, the stress value increases rapidly to 160 MPa at 2.8%.

At this stage, in addition to the elastic deformation, plastic deformation also appears to reach the elastic-plastic deformation stage. Subsequent stress values increase slowly with increasing the strain, the plastic deformation gradually increases and permanent plastic deformation of the specimen occurs, culminating in fracture. The stress value reaches a maximum of about 255 MPa at about 38% of the strain and the specimen fractures, the stress-strain curve shows a straight line downward trend. The microstructure of AZ31 after rolling deformation can vary significantly in different directions, resulting in a strong anisotropy of AZ31. However, recrystallization after annealing will make the grains fine and even, and significantly weaken the anisotropy of the anisotropy<sup>[22-23]</sup>. As shown in Fig.3, there is no significant difference in the tensile strength of the specimens in each direction, and the elongation of the specimens in each direction is also not significantly different, which is about 37%, indicating that the uniaxial tensile properties of the annealed magnesium alloy sheet have no significant anisotropy along each direction of the sheet surface. This is due to the fact that *c*-axis of most of the grains in the AZ31 magnesium alloy sheet is parallel to the ND, forming a strong base texture, and there is no significant difference in the starting ability of the slip system along each direction on the sheet surface.

**2.3 Fully reversed stress-controlled cyclic behavior**

**2.3.1 Fatigue life**

In general, the *S-N* curve can be described by Eq.(1).

$$S^m \cdot N = C \tag{1}$$

where *S* is the fatigue cycle stress, *N* is the fatigue life and *m* and *C* are material parameters.

The *S-N* curve for AZ31 magnesium alloy is shown in Fig. 4. The HCF test adopts the tension-compression symmetric loading mode, the stress ratio *R*=-1, and the loading

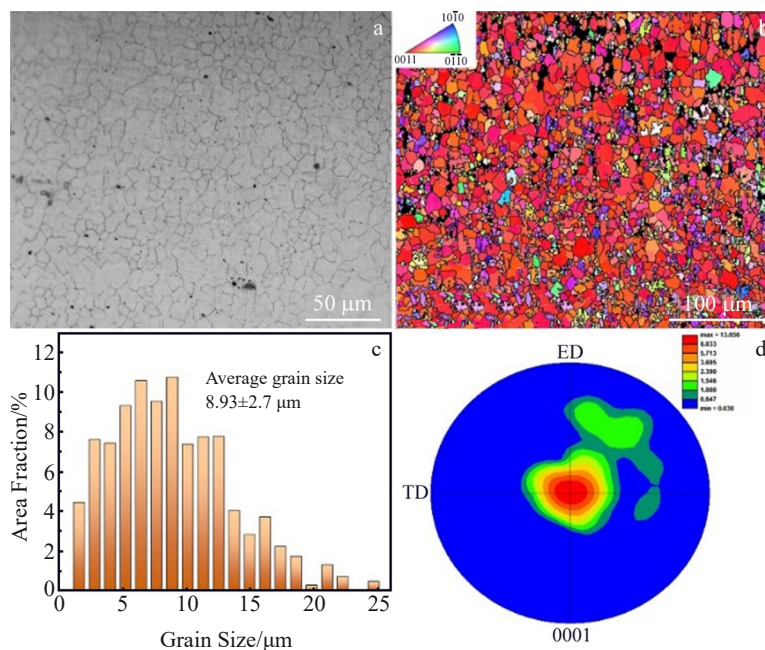


Fig.2 Metallographic image (a), EBSD map (b), grain size distribution (c), and basal (0001) planes pole figure (d) of the specimens

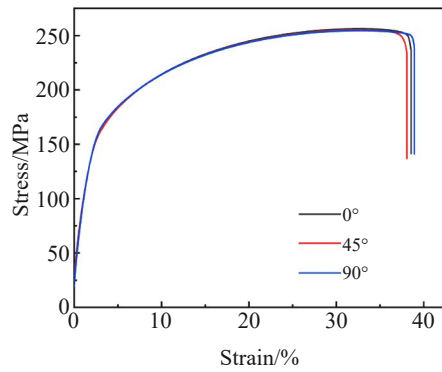


Fig.3 Stress-strain curves of AZ31 magnesium alloy under uniaxial tension in different directions

frequency is  $f=3$  Hz and  $f=30$  Hz. The fractures are all located at the middle of the scale and near the smallest cross-section of the specimen. The fatigue life of AZ31 magnesium alloy decreases with increasing cyclic stress amplitude in HCF. As can be observed in Fig.4, most of the test stress amplitudes and  $S-N$  curves for fatigue failure show a continuous decreasing trend without horizontal asymptote. When the cyclic stress amplitude is less than 90 MPa, no fracture occurs after  $10^6$  cycles. It can be seen that increasing the loading frequency from 3 Hz to 30 Hz at the same loading stress has no significant effect on fatigue life in Fig.4. This means that there is no significant frequency effect on the AZ31 in HCF test at higher cyclic stresses.

### 2.3.2 Microstructure in different cyclic stress

Fig.5 shows the microstructure of AZ31 after fatigue cycle

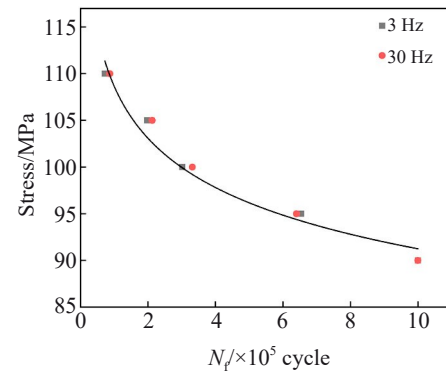


Fig.4  $S-N$  curve of rolled AZ31 magnesium alloy sheet

with different stress amplitudes at loading frequencies of  $f=3$  Hz and  $f=30$  Hz. The EBSD results show the relationship between the number of residual twins and the cyclic stress under different conditions. As shown in Fig.5a, the number of twins after cyclic loading is very small at a cycle stress of 95 MPa, and these  $\{10\bar{1}2\}$  tensile twins are different twin variants that possess different grain orientations from the parent crystal. During cyclic deformation, the characteristic microstructure of the twin shrinks inward from the boundary of the opposite twin, and tends to cut off the primary twin to form a new cell. Some of the twins split and dissociate into very small twins. In addition, the merging of the same twin variant due to twin crossing can be observed. Twins grow inward from the grain boundary and extend through the grain. The number of twins increases with the increase in cyclic stress, as shown in Fig.5b and 5c, similar evolution rules exist

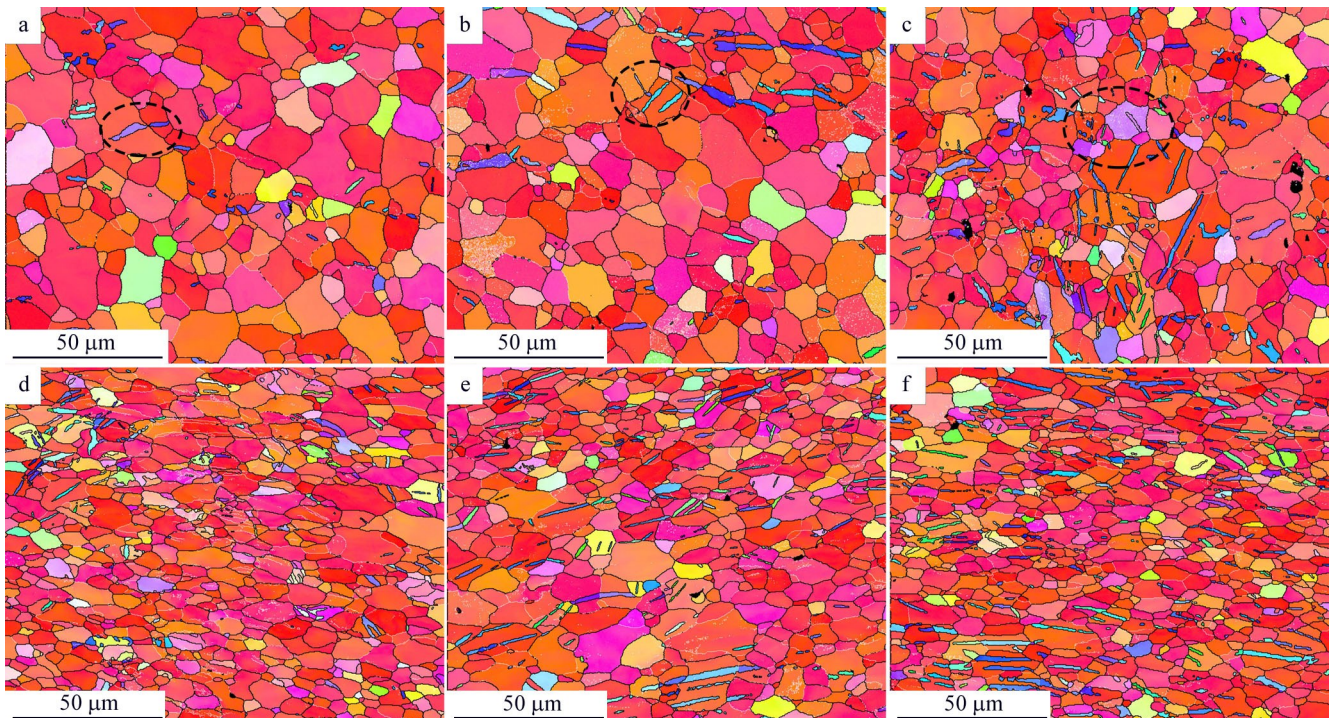


Fig.5 Microstructures of AZ31 alloy at different cyclic stresses and different frequencies: (a) 3 Hz, 95 MPa; (b) 3 Hz, 100 MPa; (c) 3 Hz, 105 MPa; (d) 30 Hz, 95 MPa; (e) 30 Hz, 100 MPa; (f) 30 Hz, 105 MPa

at different loading frequencies, and the number of twins increases with the increase in cyclic stress. Under the same stress condition, when the frequency increases from 3 Hz to 30 Hz, the number of residual twins increases, resulting in twins with different crystal orientations from the matrix, as shown in Fig.5b and 5e.

In the twinning-detwinning process, the incomplete detwinning process leads to a continuous accumulation of residual twins. The twinning produced by the twinning-detwinning behaviour changes the orientation of the original grains and can further activate slip within the region where twinning occurs, thus coordinating the fatigue deformation process.

As shown in Fig.6, the blue line is used to mark the tensile twin, the green line marks the compressive twin, and the residual twins are mainly tensile twins. The number of residual twins found in the microstructure near the fracture increases as the fatigue stress increases. Tensile twinning, basal and columnar slip, and  $\langle c+a \rangle$  conical slip are the main deformation modes of magnesium alloys. The critical shear stress (CRSS) of tensile twins is much lower than that of cylindrical and conical slip, but the degree of activation is strongly dependent on the stress amplitude. The small number of twins observed in samples with low stress cycles is due to the relatively low cyclic loading stresses during fatigue deformation, which makes it difficult to activate twinning. The deformation of fatigue crack initiation is mainly dislocation slip at low stress amplitude and twinning-detwinning process at high stress amplitude. For high-stress

cyclic samples, there are more twins, because the relatively high cyclic loading stress can produce enough deformation and provide enough energy to activate the twinning. Fatigue experiments were carried out along the RD of the sample, with most grains having their  $c$ -axis perpendicular to the RD, and the conditions for the activation of twinning are met under tensile-compression cyclic loading conditions, producing  $\{10\bar{1}2\}$  tensile twins. During subsequent tensile and compressive loading in the RD, when subjected to a load opposite to the tensile stress, it causes the base plane to rotate by  $86.3^\circ$  again and the crystal orientation to recover, at which the detwinning behaviour occurs<sup>[24]</sup>. Theoretically, the generated twins will disappear, but in practice it has been observed that the generated twins do not disappear completely and the twins observed inside the matrix after cyclic deformation are residual twins resulting from incomplete detwinning. The twinning and detwinning processes alternate throughout the cyclic loading process until fracture failure of the specimen occurs. Compression twins are also formed in grains with the right orientation during fatigue, but the stresses required to activate the compression twins are so high that there are few internal compression twins in the fatigued sample.

Fig.7 shows the texture evolution of AZ31 magnesium alloy after fatigue deformation. As shown in Fig.7a, the base texture strength of AZ31 magnesium alloy is  $\text{Max}=13.7$ . Fig.7b–7d show the microstructure of specimens under different cyclic loading stresses at a loading frequency of 3 Hz. Fig.7e–7g show the microstructure of samples under different cyclic

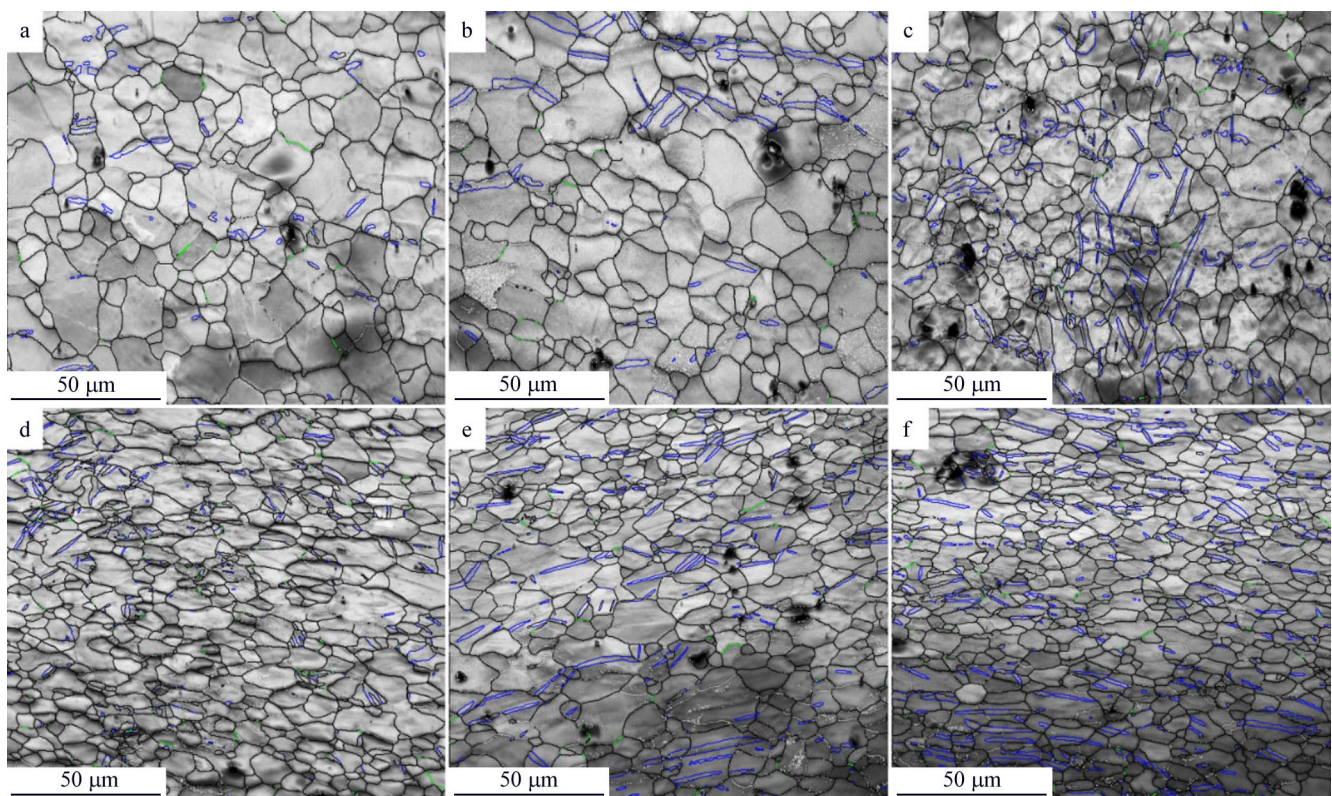


Fig.6 Twin distribution of AZ31 alloy at different cyclic stresses and different frequencies: (a) 3 Hz, 95 MPa; (b) 3 Hz, 100 MPa; (c) 3 Hz, 105 MPa; (d) 30 Hz, 95 MPa; (e) 30 Hz, 100 MPa; (f) 30 Hz, 105 MPa

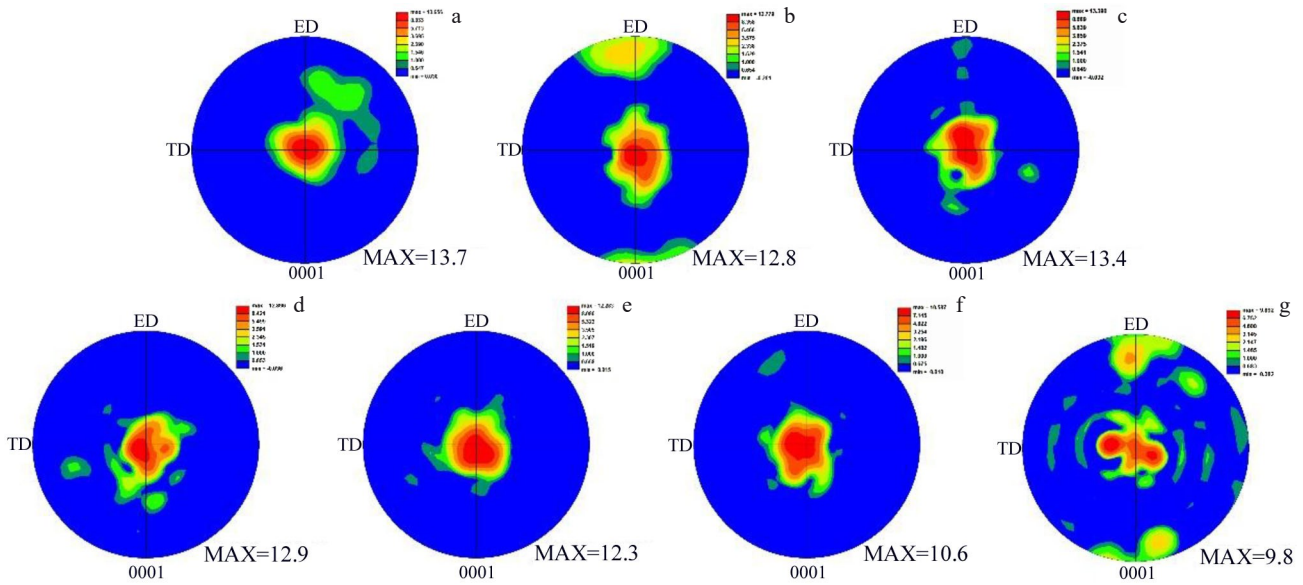


Fig.7 Microstructure evolution on (0001) of AZ31 Mg alloy under different conditions: (a) as-received; (b) 3 Hz, 95 MPa; (c) 3 Hz, 100 MPa; (d) 3 Hz, 105 MPa; (e) 30 Hz, 95 MPa; (f) 30 Hz, 100 MPa; (g) 30 Hz, 105 MPa

loading stresses at a loading frequency of 30 Hz. After fatigue deformation, the orientation distribution of the sample is more extensive, and the dispersion of the texture increases, leading to the weakening of the strength of the base texture. With the increase in cyclic stress, the base texture tends to weaken significantly (from Max=13.7 at 30 Hz to Max=9.8). The concentration of flow strain in shear zone can explain the great change of texture with the increase in loading stress. The base texture becomes weakening under high stress loading, which is due to the existence of high volume fraction of residual twins in the matrix. Therefore, with the increase in loading stress, the texture weakens significantly (Fig. 7d and 7g). The same result is obtained by Yang et al<sup>[20]</sup> where the

microscopic fatigue texture of the magnesium alloy gradually weakens with increasing cyclic loading stress.

**2.4 Fatigue fracture morphologies**

Scanning electron microscope was used to observe the macroscopic fracture morphology of fatigue fracture specimens and to determine the initiation location of fatigue cracks. Fig. 8 shows the macroscopic fracture morphology of the fatigue sample at low multiples. Red arrows and FCI are used to mark the origin of the fatigue crack, black dotted lines and FCG are used to mark the fatigue crack growth zone, and FF is used to mark the final fracture zone.

As shown in Fig.8, the crack originates near the surface of

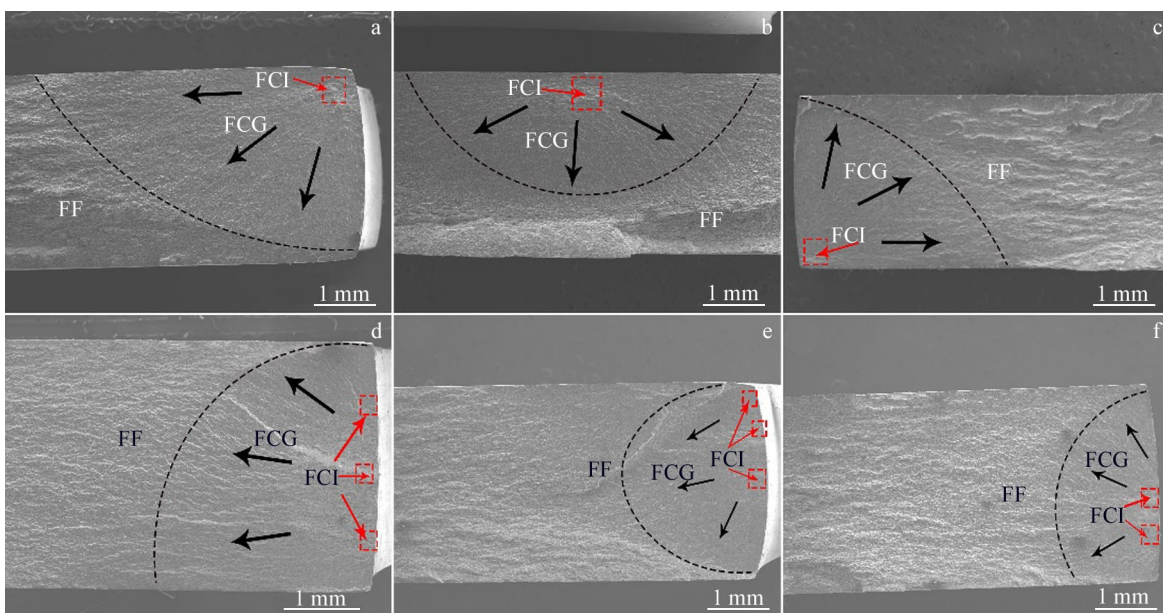


Fig.8 Macroscopic fatigue fracture of the specimens at different cyclic stresses and different frequencies: (a) 3 Hz, 95 MPa; (b) 3 Hz, 100 MPa; (c) 3 Hz, 105 MPa; (d) 30 Hz, 95 MPa; (e) 30 Hz, 100 MPa; (f) 30 Hz, 105 MPa

the sample, and the fatigue crack initiation zone and fatigue crack growth zone are relatively smooth, while the surface of the final fracture zone is rough. The results show that the fatigue cracks in all samples of AZ31 alloy are generated near the surface, and the cracks are generated on the surface of the samples and spread inward, regardless of the stress amplitude applied. Fig. 8a–8c show that when the loading frequency is low, the fatigue fracture crack initiation is characterized by a single point crack source, and finally the sample fails to fracture, forming the final fracture zone. Under the high stress amplitude, the area of crack growth zone gradually decreases with the increase in stress, because the area of crack growth

zone is proportional to the fatigue life<sup>[25]</sup>. With the gradual increase in stress, the fatigue life gradually decreases, and the increase in loading frequency also shows the same rule (Fig. 8d–8f). As shown in Fig. 8d–8f, at high frequency, the sample has obvious steps in the crack growth zone, which may be due to the non-uniform stress generated during crack growth caused by high frequency loading. In the high frequency condition shown in Fig. 8d–8f, multiple crack sources are observed on the near surface of the sample, which is related to the stress concentration location and the evolution of the internal microstructure<sup>[26]</sup>.

Fig. 9a, 9d, 9g, 9j, 9m show magnified images of the fatigue

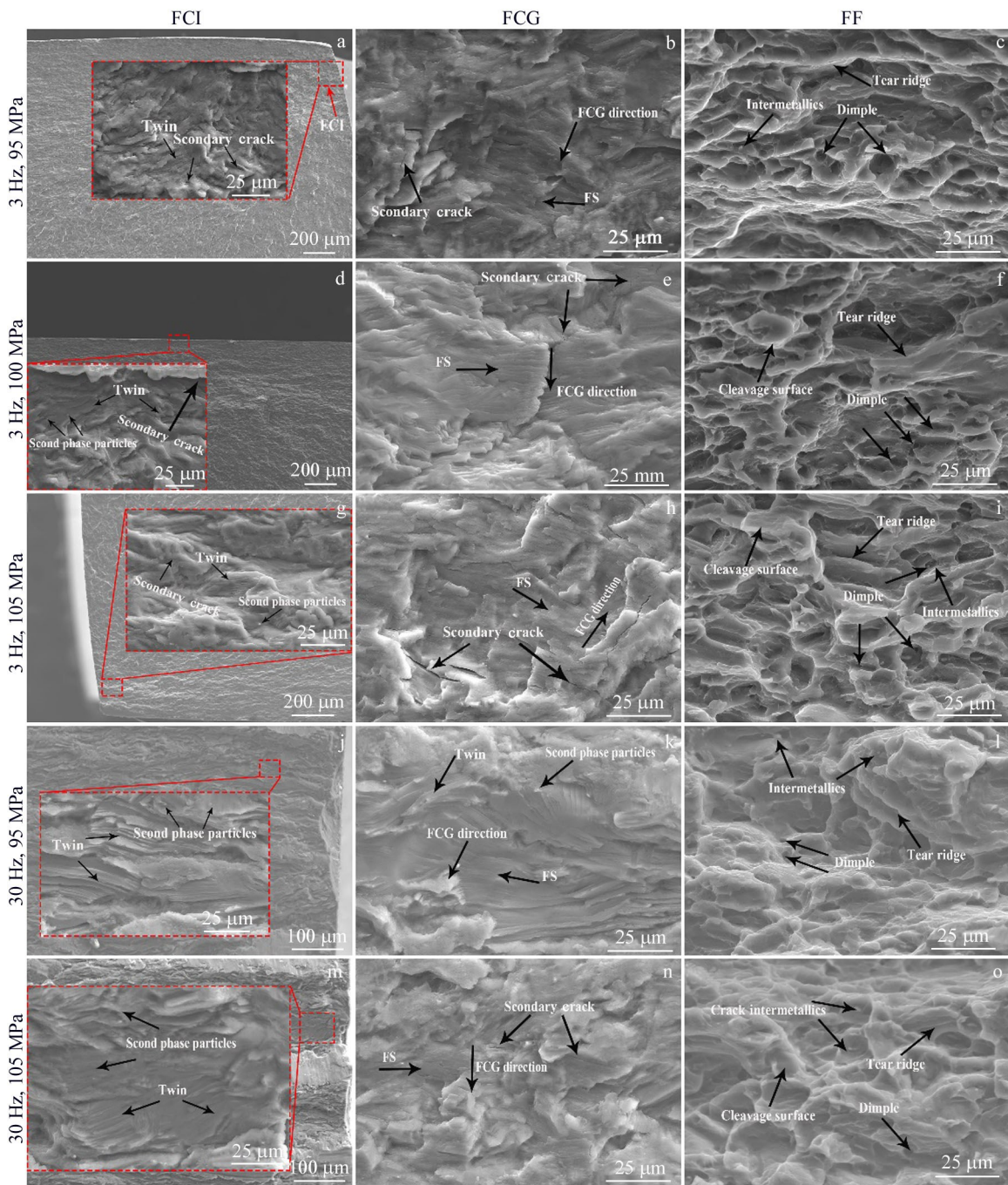


Fig.9 SEM morphologies of FCI, FCG and FF for the fatigue specimens under different conditions

crack initiation for different loading conditions. The crack source is generated near the surface of the sample, and the secondary crack, the second phase particles and the twin layer are all observed near the crack. The presence of the brittle phase ( $Mg_{17}Al_{12}$ ) is observed several times in the fatigue crack source region of the AZ series magnesium alloys<sup>[27-29]</sup>. An enlarged view of the crack source area reveals a large number of secondary cracks near the second phase, and the ridge-like shape at the crack source area is caused by the interaction of the secondary cracks at low stress amplitudes. The distribution of small planes of lath-shaped structures is found at different stress amplitudes, and these lath-shaped structures are mainly twinned during cyclic loading deformation, in agreement with previous microstructural analyses that the twin boundaries of irreversible twinning and dislocations generated in the second phase during fatigue deformation significantly influence crack generation at high stress amplitudes. As the cyclic loading process proceeds, crack expansion reaches a critical size where instantaneous fracture occurs, forming a final fracture zone with a rough surface, as shown in Fig. 9c, 9f, 9i, 9l, 9o. As can be seen in Fig. 9, the transient fracture zone of the fatigue fracture is similar to the quasi-static tensile fracture morphology, with typical fracture morphology features such as dimple, tear ribs, deconstruction surfaces and a small number of secondary cracks observed. The twinning-detwinning behaviour during cyclic loading leads to the generation of a large number of residual twins.

### 3 Conclusions

1) With the gradual increase in cyclic loading stresses, a gradual increase in the number of residual twins is observed in the fatigue specimens of AZ31 magnesium alloy at different loading frequencies, and the main residual twins are  $\{10\bar{1}2\}$  tensile twins. Under the same cyclic loading conditions, the number of residual twins increases at higher loading frequencies. Tensile twinning induces recrystallization during cycling, and the grains gradually refine as the stress amplitude increases.

2) Rolled AZ31 magnesium alloy sheets have a strong basal texture with a strength of  $MAX=13.7$ . With increasing stress amplitude and loading frequency, the basal texture of AZ31 magnesium alloy tends to weaken significantly, which is related to the residual twins generated during cyclic loading deformation. A minimum basal texture strength of  $MAX=9.8$  is obtained at 30 Hz, 105 MPa.

3) The fatigue fracture of AZ31 magnesium alloy is typical in different loading frequencies ( $f=3$  Hz and  $f=30$  Hz) and stress conditions. As the stress amplitude increases, the area of the fatigue extension zone decreases and the fatigue life decreases. At a loading frequency of  $f=30$  Hz, the number of crack sources gradually increases, the surface of the crack sprouting zone becomes rough and irregular, and the area of the fatigue extension zone decreases compared to that at  $f=3$  Hz.

4) An increase in the number of twin layers is observed in

the crack sprouting zone at the loading frequency of  $f=30$  Hz, the area of the crack extension zone decreases, and the surface of the crack extension zone becomes rough and uneven. Obvious fatigue growth lines are observed in the specimens with different loading conditions, and the morphology of the final fatigue fracture zone is mainly tough dimples, and the size of the tough dimples increases with the increase in stress at  $f=3$  Hz. At  $f=3$  Hz, the number and size of the tough dimples decreases and the number of the solution planes increases, showing a typical mixed fracture morphology.

### References

- 1 Hono K. *Scripta Metallurgica et Materialia*[J], 1994, 30(6): 695
- 2 Froes F H. *Materials Science and Engineering A*[J], 1994, 184(2): 119
- 3 Mayyas A, Omar M, Hayajneh M et al. *Journal of Cleaner Production*[J], 2017, 167(20): 687
- 4 Mordike B L, Ebert T. *Materials Science and Engineering A*[J], 2001, 302(1): 37
- 5 Luo A A. *Journal of Magnesium and Alloys*[J], 2013, 1(1): 2
- 6 Joost, William J. *Scripta Materialia*[J], 2017, 128: 107
- 7 Weiler J P. *Journal of Magnesium and Alloys*[J], 2019, 7(2): 297
- 8 Kabirian F, Mahmudi R. *Metallurgical and Materials Transactions A*[J], 2010, 41: 3488
- 9 Wen K B, Wang F, Jin L et al. *Materials Science & Engineering A*[J], 2016, 667: 171
- 10 Matsuzuki M, Horibe S. *Materials Science & Engineering A*[J], 2009, 504(1-2): 169
- 11 Xu D K, Han E H. *Scr Mater*[J], 2013, 69: 702
- 12 Yang F, Yin S M, Li S X et al. *Materials Science & Engineering A*[J], 2008, 491(1): 131
- 13 Uematsu Y, Tokaji K, Kamakura M et al. *Materials Science & Engineering A*[J], 2006, 434: 131
- 14 Tokaji K, Kamakura M, Ishiizumi Y et al. *International Journal of Fatigue*[J], 2004, 26: 1217
- 15 Yin S M, Yang H J, Li S X et al. *Scripta Materialia*[J], 2008, 58(9): 751
- 16 Koike J, Fujiyama N, Ando D et al. *Scripta Materialia*[J], 2010, 63(7): 747
- 17 Abbas Jamali, Anxin Ma, Javier Lorca. *Scripta Materialia*[J], 2022, 207: 114 304
- 18 Trojanova, Zuzanka, Chalupova et al. *International Journal of Materials Research*[J], 2016, 107(10): 903
- 19 Yu D L, Zhang D F, Luo Y X et al. *Materials Science & Engineering A*[J], 2016, 658: 99
- 20 Yang F, Yin S M, Li S X et al. *Materials Science and Engineering A*[J], 2008, 491(1): 131
- 21 Jordon J B, Brown H R, Kadiri H E et al. *International Journal of Fatigue*[J], 2013, 51(51): 8
- 22 Li Xianrong, Mi Yujie, Nie Huihui et al. *Rare Metal Materials and Engineering*[J], 2020, 49(1): 320
- 23 Zhao Xi, Gao Pengcheng, Zhang Zhimin et al. *International*



- Journal of Fatigue[J], 2020, 132: 105-393
- 24 Aps A, Sn B, Mab A et al. *Materialia*[J], 2021, 20: 101-219
- 25 Xiong Y, Yu Q, Jiang Y. *International Journal of Plasticity*[J], 2014, 53: 107
- 26 Gryguc A, Shaha S K, Behravesh S B et al. *International Journal of Fatigue*[J], 2017, 104: 136
- 27 Gryguc A, Behravesh S B, Shaha S K. *International Journal of Fatigue*[J], 2018, 116: 429
- 28 Gryguć A, Behravesh S B, Shaha S K. *International Journal of Fatigue*[J], 2019, 127: 324
- 29 Culbertson D, Jiang Y. *Materials Science & Engineering A*[J], 2016, 676: 10

## AZ31 镁合金在高周疲劳过程中微观组织和孪晶演变特征

杨福来<sup>1</sup>, 王 强<sup>2</sup>, 张 峥<sup>1</sup>

(1. 北京航空航天大学 材料科学与工程学院, 北京 100191)

(2. 中北大学 材料科学与工程学院, 山西 太原 030051)

**摘 要:** 利用扫描电子显微镜 (SEM) 和电子背散射衍射 (EBSD) 技术研究了室温条件下 AZ31 镁合金在不同加载频率 (3 和 30 Hz) 和不同应力幅值 (90, 95, 100, 105, 110 MPa) 疲劳变形后的组织演变规律及断口形貌特征。结果表明: 随着加载应力增加, 基体内残余孪晶数量增加, 残余孪晶主要以  $\{10\bar{1}2\}$  拉伸孪晶形式存在。随着应力幅值的增加晶粒逐渐细化, 这是由于在循环过程中, 拉伸孪晶演变诱导晶粒细化。随着应力幅值的增加, 织构强度显著减弱, 这与试样疲劳后的再结晶机制有关。通过对试样疲劳断口的分析, 发现孪晶片层处容易引起裂纹萌生, 随着应力的增加, 试样中裂纹扩展区面积逐渐减小, 在疲劳裂纹扩展区观察到明显的疲劳辉纹。最终断裂区表面粗糙, 主要存在韧窝、撕裂脊以及二次裂纹等形貌。在最终断裂区可观察到韧窝, 韧窝尺寸随着循环应力的增加, 在较高加载频率下, 韧窝的尺寸与数量均减小。

**关键词:** AZ31 镁合金; 疲劳变形; 孪晶; 微观组织; 断口形貌

作者简介: 杨福来, 男, 1996年生, 博士生, 北京航空航天大学材料科学与工程学院, 北京 100191, E-mail: buaayangfulai@163.com